Ultrasonic wave effects on the diameter of TiO_2 nanoparticles

Authors:
Hossain Milani Moghaddam[1,2,3]
Shahruz Nasirian[1,2,4]

Affiliations:
[1]Physics Department, Mazandaran University, Babolsar, Iran

[2]Molecular Electronics Lab, Physics Department, Mazandaran University, Babolsar, Iran

[3]Nano and Biotechnology Group, Faculty of Basic Sciences, Mazandaran University, Babolsar, Iran

[4]Basic Sciences Department, University of Science and Technology of Mazandaran, Babol, Iran

Correspondence to:
Hossain Milani Moghaddam

email:
milani@umz.ac.ir

Postal address:
PO Box 416, Physics Department, Mazandaran University, Pasdaran Street, Babolsar, Mazandaran, Iran

Dates:
Received: 04 Aug. 2010
Accepted: 08 Dec. 2010
Published: 14 Mar. 2011

How to cite this article:
Milani Moghaddam H, Nasirian S. Ultrasonic wave effects on the diameter of TiO_2 nanoparticles. S Afr J Sci. 2011;107(3/4), Art. #389, 5 pages. DOI: 10.4102/sajs.v107i3/4.389

Titanium dioxide (TiO_2) nanostructured materials have attracted a great deal of attention because of their numerous applications. However, TiO_2 applications depend strongly on the material's high homogeneity and definite phase composition, morphology, particle size, high surface area and porosity, which are dependent on the sample history, the method of preparation and heat treatment. We synthesised TiO_2 nanopowder with an anatase structure by the sol-gel method using $TiCl_4$-ethanol solution as a precursor in an argon gas environment, with and without applying ultrasonic waves. Our results show that the use of ultrasonic waves (after aging) has a significant effect on the homogeneity and size of TiO_2 nanoparticles. A smaller crystallite size was obtained using ultrasonic waves. For this purpose, the average diameter of TiO_2 nanoparticles was decreased by about 3 nm. The synthesised powder was characterised by X-ray diffraction, scanning electron microscopy and transmission electron microscopy.

Introduction

Titanium dioxide (TiO_2) nanostructured materials have attracted a great deal of attention because of their numerous applications in various fields, such as in photocatalysts and self-cleaning,[1,2] dye-sensitised solar cells,[3,4,5,6] gas sensing and sensor devices,[7,8] electroluminescent hybrid devices,[9] energy-storage technologies,[10] electrodes in lithium batteries[11] and water-splitting catalysts for generating hydrogen.[12,13] TiO_2 has recently been tested as a dielectric material for the next generation of ultrathin capacitors[14] and as a photonic crystal for photonic band-gap materials.[15,16] TiO_2 has three main structures: rutile, anatase and brookite.[17,18,19] The anatase phase of TiO_2 is useful in photocatalytic applications because of its higher electron mobility, lower fixed dielectric properties and lower density than the other phases.[17,20]

TiO_2 applications depend strongly on the material's high homogeneity and definite phase composition,[21] morphology, particle size, high surface area and porosity.[19,20,22,23] All of the above parameters depend on the sample history,[24] the method of preparation[25] and the heat treatment used.[26] Some parameters play a more important role than others. For example, the size or surface area to volume ratio of the nanoparticles is an important factor for their application in catalysis.[20,27,28] Thus, it is very important to develop synthetic methods in which the crystalline phase as well as the size and morphology of the TiO_2 nanocrystals can be controlled. Having fine and homogeneous nanoparticles with controlled diameters is necessary for using this material as a good photocatalyst.[17,20,29]

TiO_2 nanoparticles can be synthesised using various methods, such as the sulphate process,[30] the chloride process,[30] impregnation,[31] co-precipitation,[32] the hydrothermal method,[33,34,35] direct oxidation of $TiCl_4$,[36] the metal organic chemical vapour deposition method[37] and the sol-gel method.[38,39] The sol-gel method is one of the most convenient ways to synthesise various metal oxides because of its low cost, ease of fabrication and low processing temperatures.[40] It is worth mentioning that only a few investigations have so far dealt with a comparison between the crystallisation process of TiO_2 in the presence or absence of ultrasonic irradiation after gelatinisation with the sol-gel method. Some investigations have recently used ultrasonic irradiation in the crystallisation process of TiO_2.[22,23,41,42,43,44,45,46,47,48,49]

In the present work, TiO_2 nanoparticles (anatase phase) were synthesised using the sol-gel process on their $TiCl_4$ precursor both with and without ultrasonic irradiation at 40 kHz (low intensity) and for specific gelatinisation times. Here, we compare the size and morphology of the particles in the presence and absence of ultrasonic irradiation.

Experimental set-up

$TiCl_4$ (99.5% Merck, Hohenbrunn, Germany) and ethanol solutions (99.8% Merck, Darmstadt, Germany) with a certain ratio in an argon gas environment were used without any further purification. All of the chemicals were analytical grade.

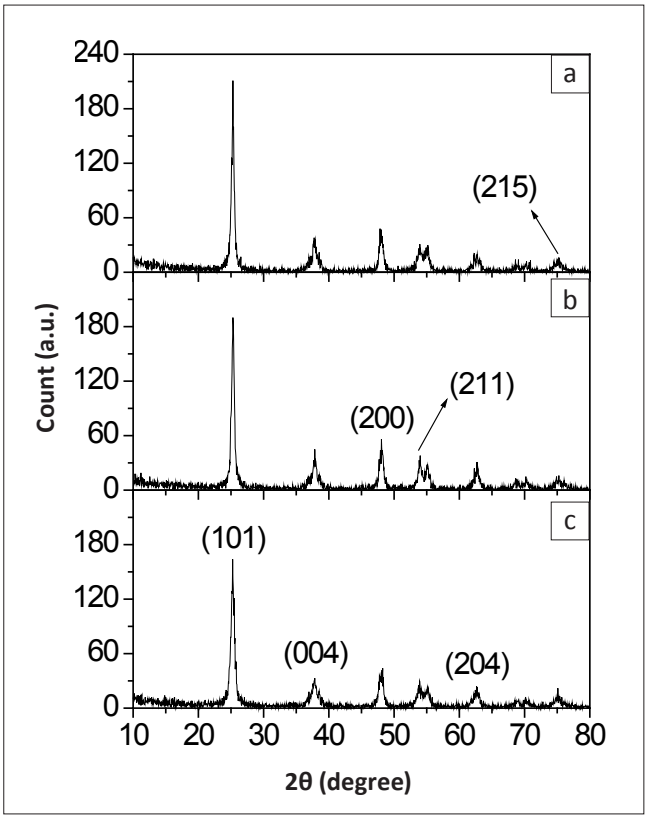

FIGURE 1: X-ray diffraction patterns for TiO_2 powder samples synthesised at a calcination temperature of 400 °C and gelatinisation times of (a) 120 h, (b) 72 h and (c) 24 h, in the absence of ultrasonic waves.

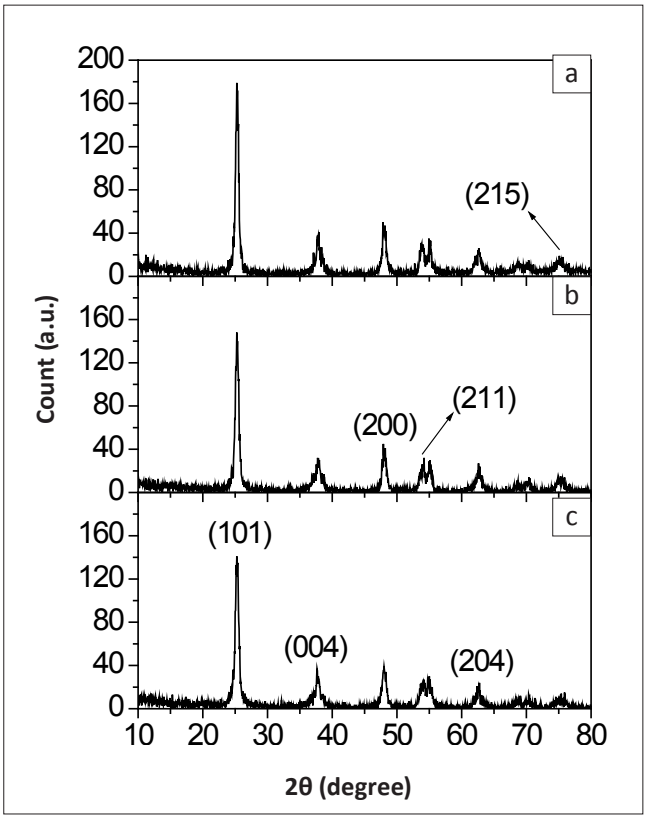

FIGURE 2: X-ray diffraction patterns for TiO_2 powder samples synthesised at a calcination temperature of 400 °C and gelatinisation times of (a) 120 h, (b) 72 h and (c) 24 h, in the presence of ultrasonic waves.

At room temperature under argon gas, 2 ml of $TiCl_4$ was slowly added drop wise into 20 ml of ethanol. A light yellow solution was obtained after adding all the $TiCl_4$. The pH value of the solution was between 1.5 and 2.0. The solution was then gelatinised for different periods (24 h, 72 h and 120 h) and each prepared solution was subjected to an aging process for 3 h. We prepared each gel solution in two ways, (1) without using ultrasonic waves and (2) with ultrasonic waves at a frequency of 40 kHz and a power of 60 W for 30 min. Each sol-gel solution was vaporised at 80 °C until a dry gel was obtained. Finally, the dry-gel precursor was calcined at 400 °C for 1 h in air to form TiO_2 powder. To promote the decomposition of organic components in the precursor, the initial heating rate was maintained at 5°C/min.

Phase identification and crystallite size determination of the products were achieved using X-ray diffraction (XRD)[17,18,19,20,21,22] on a GBC-MMR diffractometer (Melbourne, Australia) at a scan rate of 10°/min and Cu–Kα line (λ = 0.1541056 nm) radiation with a working voltage of 30 kV. The particle morphology was investigated using a Philips XL30 scanning electron microscope (Eindhoven, the Netherlands) and a Philips CM120 transmission electron microscope[50] operating at 16 kV and 100 kV, respectively.

Results and discussion

Using the sol-gel method, the diameter of TiO_2 nanoparticles can be controlled by adjusting several physical and chemical factors, such as gelatinisation time and calcination temperature,[17,18] and other methods can be used for reducing the size of the particles.

In order to synthesise TiO_2 nanoparticles, one can combine $TiCl_4$ and ethanol under special conditions. At first a large amount of HCl gas and $TiCl_x(OH)_{4-x}$ is produced in combining $TiCl_4$ and ethanol. In the mixing process, the solution $TiCl_x(OH)_{4-x}$ absorbs a small amount of water from the atmosphere and forms Ti-OH bonds with the remaining ethanol in the solution. In the polymerisation and hydrolysis process, these Ti-OH bonds form …-Ti-O-…-Ti-OH strings. In the hydrolysis process and while mixing, these long strings form smaller Ti-O-Ti strings. In closing and with development of Ti-O-Ti strings, three-dimensional polymers are produced to form $Ti(OH)_4$ matter. TiO_2 nanoparticles are formed when $Ti(OH)_4$ molecules are under specific (critical) thermal conditions according to the following equation[17,18,29]:

$$Ti(OH)_4 \rightarrow TiO_2 + 2H_2O \qquad \text{[Eqn 1]}$$

The …-Ti-O-…-Ti-OH strings break and produce a large number of smaller Ti-O-Ti strings, which help to form more $Ti(OH)_4$ molecules. The $Ti(OH)_4$ molecules emerging at a high rate in solution cause the formation of more TiO_2 nanoparticles in a short time.

Ultrasonic waves have a monotonous effect on all components of the solution made by the sol-gel method and cause the breaking of loose links of large nanometric

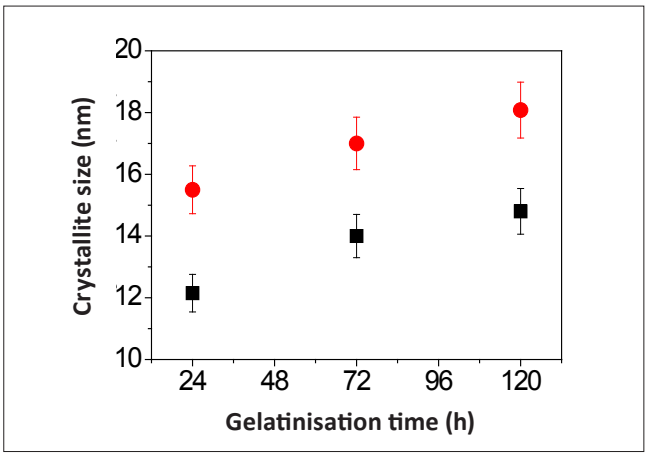

FIGURE 3: Crystallite size at different gelatinisation times after calcination for 1 h at 400 °C with (squares) and without (circles) ultrasonic irradiation.

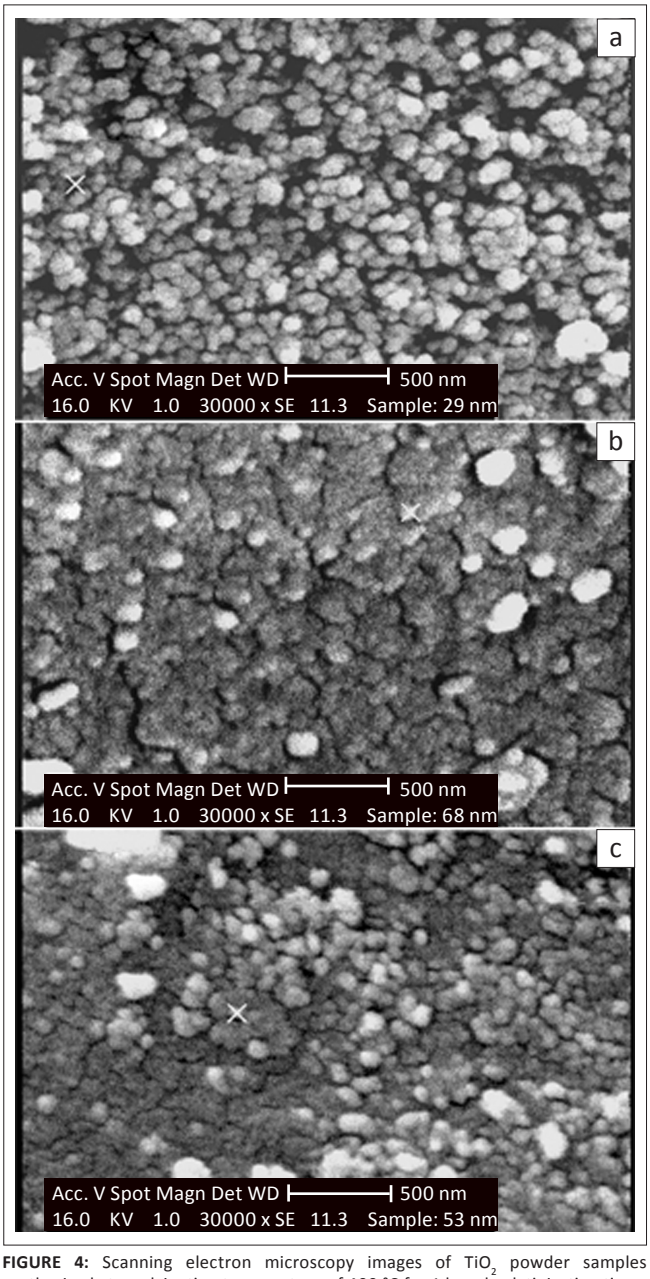

FIGURE 4: Scanning electron microscopy images of TiO_2 powder samples synthesised at a calcination temperature of 400 °C for 1 h and gelatinisation times of (a) 120 h, (b) 72 h and (c) 24 h, in the presence of ultrasonic waves.

colloids in solution, thus allowing the production of smaller nanoparticles. The high local pressure and temperature break the links in long polymer strings as well as the weak links binding smaller particles that form large colloidal masses. Very small bubbles are produced in the fluid when it is affected by ultrasonic waves. These bubbles collapse when they grow beyond a critical size and this creates high temperatures of 5000 °K and pressures of 10^8 Pa in the area of collapse. The ultrasonic waves create three distinct states within the fluid, (1) that inside the bubbles (in their gaseous phase) where extremely high temperatures and pressures are produced as they collapse; (2) spaces between the bubbles within the fluid, where temperature is less than that inside the bubbles but is still high; and (3) the overall volume of fluid, where temperatures are equal to the ambient temperature.[17] As the bubbles collapse, there is a high heating to cooling rate of about 10^{10} K/s – 10^{11} K/s in the boundaries between the bubbles and fluid (active area). It was found that applying ultrasonic waves after the gel solution has been mixed is an ideal technique to reduce the diameter of the TiO_2 nanoparticles formed.

The samples prepared at different gelatinisation times (24 h, 72 h and 120 h) and calcined at 400 °C were compared using XRD. Phase identification using XRD relies mainly on the position of the peaks in a diffraction profile and to some extent on the relative intensities of these peaks.[17,18,19,20,21,22,40] The half width of the peaks decreases slightly when the size of the crystallites decreases. Figures 1 and 2 show the XRD patterns for powder samples of TiO_2 obtained at a calcination temperature of 400 °C and gelatinisation times of 24 h, 72 h and 120 h, with and without ultrasonic waves, respectively. All the observed peaks in the XRD spectra are related to the anatase phase. In Figure 2, the crystallite diameters relative to those in Figure 1 were estimated for most sharp peaks using Debye-Scherrer's equation:

$$S=K.\lambda/(\beta \cos\theta) \qquad [Eqn\ 2]$$

where S is the crystallite size, λ = 1.54056 Å (the wavelength of the X-ray radiation), K is a constant taken as 0.94, θ is the diffraction half angle and β is the line width at half maximum height.

Figure 3 and Table 1 show a comparison of the average diameter of synthesised crystallites with and without the use of ultrasonic waves. The crystallite dimensions evaluated from the line profile analysis of the XRD peaks indicated that all prepared samples were nanocrystalline in the anatase phase and that crystallites with a mean diameter of less than 15 nm were prepared in the presence of ultrasonic waves. By applying ultrasonic waves, the average diameter of the TiO_2 nanoparticles was reduced by about 3 nm during each gelatinisation time of 24 h, 72 h and 120 h.

Both Figure 1 and Figure 2 show that, as gelatinisation time increases, the beam plates' diffraction peak of the anatase phase becomes sharper and the line width at half maximum

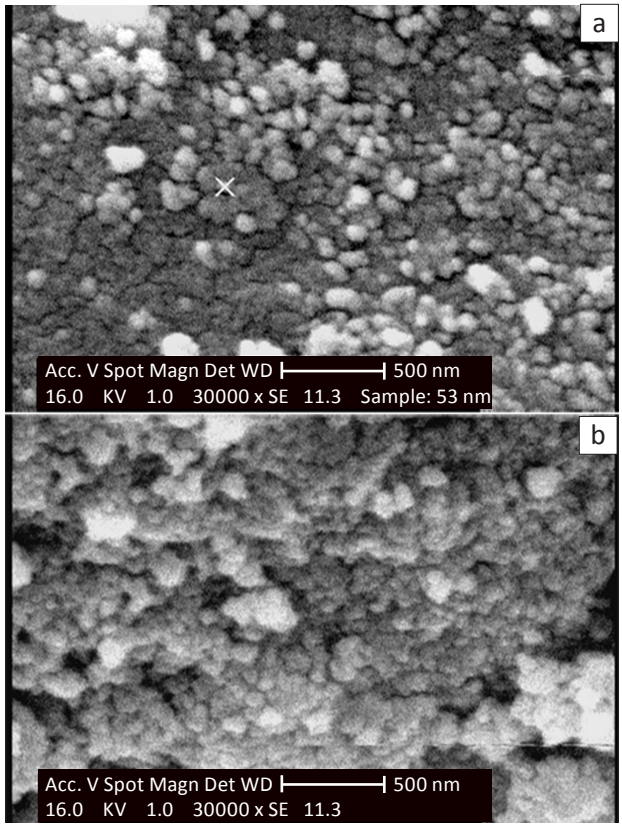

FIGURE 5: Scanning electron microscopy images of TiO_2 powder samples synthesised at a calcination temperature of 400 °C for 1 h and a gelatinisation time of 24 h (a) in the presence of and (b) in the absence of ultrasonic irradiation.

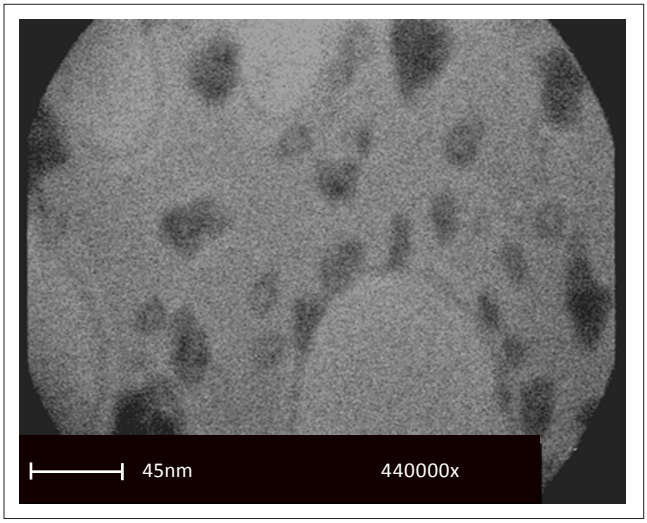

FIGURE 6: Transmission electron microscopy image of TiO_2 powder samples synthesised at a calcination temperature of 400 °C for 1 h and a gelatinisation time of 120 h in the presence of ultrasonic irradiation.

TABLE 1: TiO_2 powder samples synthesised under different conditions at a calcination temperature of 400 °C.

Gelatinisation time (h)	Crystallite size (nm) using ultrasonic waves	Crystallite size (nm) without using ultrasonic waves	Phase
24	12.15	15.50	anatase
72	14.00	17.00	anatase
120	14.80	18.08	anatase

height decreases. Therefore, by increasing the gelatinisation time, the size of the crystallites became larger. Figure 4 shows scanning electron microscope (SEM) images of TiO_2 powder samples prepared using ultrasonic waves and different gelatinising times. With increased gelatinisation time, the boundaries between the nanometric grains became more specific and the shape of the particles became more spherical.

Figure 5 compares SEM images of TiO_2 powder samples prepared using a gelatinisation time of 24 h, with and without ultrasonic waves. The images of the surface of the powder samples show clearly that using ultrasonic waves resulted in greater homogeneity in the average size of the particles and resulted in smaller particles. Transmission electron microscopy (TEM) also was used to investigate the particle size. Figure 6 shows a TEM image of nanoparticles synthesised using a gelatinisation time of 120 h, a calcination temperature of 400 °C and ultrasonic waves. The nanoparticles produced had a diameter of 14 nm – 15 nm.

The above results show that if gelatinisation times are increased, the average size of TiO_2 nanoparticles increases, irrespective of whether or not ultrasonic waves are applied. In addition, if ultrasonic waves are used, the average diameter of TiO_2 nanoparticles decreases by about 3 nm. Thus, smaller and more controlled nanoparticles can be produced using ultrasonic waves.

Conclusion

We successfully prepared TiO_2 nanoparticles using $TiCl_4$ and ethanol as precursors by a sol-gel route, in the presence and absence of ultrasonic waves at room temperature. The use of ultrasonic waves led to smaller particle size, low-dimensional particle shape (spherical) and improved particle morphology. The fact that nanoparticles can be produced using ultrasonic waves, as reported in this paper, strongly supports the proposition that ultrasonic irradiation has great potential to control the formation of inorganic nanoparticles by influencing the organic reaction pathway.

References

1. Fujishima A, Honda K. Electrochemical photolysis of water at a semiconductor electrode. Nature. 1972;238:37–38. doi:10.1038/238037a0, PMid:12635268
2. Trung T, Ha CS. One-component solution system to prepare nanometric anatase TiO_2. Mater Sci Eng. 2004;C(24):19–22.
3. O'Regan B, Grätzel M. A low-cost, high-efficiency solar cell based on dye-sensitized colloidal TiO_2 films. Nature. 1991;353:737–740. doi:10.1038/353737a0
4. Adachi M, Murata Y, Takao J, Jiu J, Sakamoto M, Wang F. Highly efficient dye-sensitized solar cells with a titania thin-film electrode composed of a network structure of single-crystal-like TiO_2 nanowires made by the "oriented attachment" mechanism. J Am Chem Soc. 2004;126:14943–14949. doi:10.1021/ja048068s, PMid:15535722
5. Dürr M, Schmid A, Obermaier M, Rosselli S, Yasuda A, Nelles G. Low-temperature fabrication of dye-sensitized solar cells by transfer of composite porous layers. Nat Mater. 2005;4:607–611. doi:10.1038/nmat1433, PMid:16041379
6. Wang W, Gu B, Liang L, Hamilton WA, Wesolowski DJ. Synthesis of rutile (a-TiO_2) nanocrystals with controlled size and shape by low-temperature hydrolysis: Effects of solvent composition. J Phys Chem. 2004;B(108):14789–14792.
7. Skubal LR, Meshkov NK, Vogt MC. Detection and identification of gaseous organics using a TiO_2 sensor. J Photochem Photobiol. 2002;A(148):103–108.

8. Meier KR, Gratzel M. Redox targeting of oligonucleotides anchored to nanocrystalline TiO_2 films for DNA detection. ChemPhysChem. 2002;3:371–374. doi:10.1002/1439-7641(20020415)3:4<371::AID-CPHC371>3.0.CO;2-O
9. Thelakkat M, Schmitz C, Schmidt HW. Fully vapor-deposited thin-layer titanium dioxide solar cells. Adv Mater. 2002;14:577–581. doi:10.1002/1521-4095(20020418)14:8<577::AID-ADMA577>3.0.CO;2-S
10. Lim SH, Luo J, Zhong Z, Ji W, Lin J. Room-temperature hydrogen uptake by TiO_2 nanotubes. Inorg Chem. 2005;44:4124–4126. doi:10.1021/ic0501723, PMid:15934734
11. Kavan L, Grätzel M, Rathousky J, Zukal A. Nanocrystalline TiO_2 (anatase) electrodes: Surface morphology, adsorption and electrochemical properties. J Electrochem Soc. 1996;143:394–400. doi:10.1149/1.1836455
12. Khan SUM, Al-Shahry M, IngLer WB. Efficient photochemical water splitting by a chemically modified n-TiO_2. Science. 2002;297:2243–2245. doi:10.1126/science.1075035, PMid:12351783
13. Park JH, Kim S, Bard AJ. Novel carbon-doped TiO_2 nanotube arrays with high aspect ratios for efficient solar water splitting. NanoLett. 2006;6:24–28. doi:10.1021/nl051807y, PMid:16402781
14. Gonzalez RJ, Zallen R, Berger H. Infrared reflectivity and lattice fundamentals in anatase TiO_2. Phys Rev. 1997;B(55):7014–7017.
15. Jiang X, Herricks T, Xia Y. Monodispersed spherical colloids of titania: Synthesis, characterization, and crystallization. Adv Mater. 2003;15:1205–1209. doi:10.1002/adma.200305105
16. Wijnhoven G, Vos WL. Preparation of photonic crystals made of air spheres in titania. Science. 1998;281:802–804. doi:10.1126/science.281.5378.802
17. Xiaobo C, Mao SS. Titanium dioxide nanomaterials: Synthesis, properties, modifications and application. Chem Rev. 2007;107:2891–2906. doi:10.1021/cr0500535, PMid:17590053
18. Zhu Y, Zhang L, Gao C, Cao L. The synthesis of nanosized TiO_2 powder using a sol-gel method $TiCl_4$ as a precursor. J Math Sci. 2000;35:4049–4054. doi:10.1023/A:1004882120249
19. Mahshid S, Askari M, Sasani Ghamsari M. Synthesis of TiO_2 nanoparticles by hydrolysis and peptization of titanium isopropoxide solution. J Mater Process Technol. 2007;189:296–300. doi:10.1016/j.jmatprotec.2007.01.040
20. Kaneko M, Okura I. Photocatalysis science and technology. Berlin/Heidelberg/New York: Kodansha/Springer Press, 2002; p. 57–260.
21. Tang Z, Zhang J, Cheng Z, Zhang Z. Synthesis of nanosized rutile TiO_2 powder at low temperature. Mater Chem Phys. 2002;77:314–317. doi:10.1016/S0254-0584(02)00003-2
22. Guo W, Lin Z, Wang X, Song G. Sonochemical synthesis of nanocrystalline TiO_2 by hydrolysis of titanium alkoxides. Microelectron Eng. 2003;66:95–101. doi:10.1016/S0167-9317(03)00031-5
23. Ramaswamy V, Jagtap NB, Vijayanand S, Bhange DS, Awati PS. Photocatalytic decomposition of methylene blue on nanocrystalline titania prepared by different methods. Mater Res Bull. 2008;43:1145–1152. doi:10.1016/j.materresbull.2007.06.003
24. Morales BA, Novaro O. Effect of hydrolysis catalyst on the Ti deficiency and crystallite size of sol-gel TiO_2 crystalline phases. J Mater Res. 1995;10:2788–2796. doi:10.1557/JMR.1995.2788
25. Nam HJ, Amemiya T, Murabayashi M, Itoh K. Photocatalytic activity of sol-gel TiO_2 thin films on various kinds of glass substrates: The effects of Na+ and primary particle size. J Phys Chem. 2004;B(108):8254–8259.
26. Yoldas BE. Hydrolysis of aluminium alkoxides and bayerite conversion. J Appl Chem Biotechnol. 1973;23:803–809. doi:10.1002/jctb.5020231103
27. Pal M, Garcia Serrano J, Santiago P, Pal U. Size-controlled synthesis of spherical TiO_2 nanoparticles: Morphology, crystallization, and phase transition. J Phys Chem. 2007;C(111):96–102.
28. Lee KM, Suryanarayanan V, Ho KC. The influence of surface morphology of TiO_2 coating on the performance of dye-sensitized solar cells. Sol Energy Mater Sol Cells. 2006;90:2398–2404. doi:10.1016/j.solmat.2006.03.034
29. Brinker J, Scherer GW. Sol-gel science. 1st ed. San Diego: Academic Press, 1990; p. 50–720.
30. Grant MH, Othmer K. Hydrogen sulfide in toxicology of the eye. Encycl Chem Technol. 1997;24:225–229.
31. Litter MI, Navio JA. Photocatalytic properties of iron-doped titania semiconductors. J Photochem Photobiol A Chem. 1994;84:171–181.
32. Palmisano L, Augugliaro V, Sclafani A, Schiavello M. Activity of chromium-ion-doped titania for the dinitrogen photoreduction to ammonia and for the phenol photodegradation. J Phys Chem. 1988;92:6710–6713. doi:10.1021/j100334a044
33. Wang Y, Cheng H, Hao Y, Ma J, Li W, Cai S. Characterization and photo-electric behaviors of Fe(III) doped TiO_2 nanoparticles. J Mater Sci. 1999;34:3721–3729. doi:10.1023/A:1004611724069
34. Cheng H, Ma J, Zhao Z, Qi L. Hydrothermal preparation of uniform nanosize rutile and anatase particles. Chem Mater. 1995;7:663–671. doi:10.1021/cm00052a010
35. Wang Y, Hao Y, Cheng H, et al. The photoelectrochemistry of transition metal-ion-doped TiO_2 nanocrystalline electrode and higher solar cell conversion efficiency based on Zn^{+2}-doped TiO_2 electrode. J Mater Sci. 1999;34:2773–2779. doi:10.1023/A:1004658629133
36. Akhtar MK, Xiong Y, Pratsinis SE. Vapor synthesis of titania powder by titanium tetrachloride oxidation. AIChE J. 1991;37:1561–1570. doi:10.1002/aic.690371013
37. Ding Z, Hu X, Lu GQ, Yue PL, Greenfield PF. Novel silica gel supported TiO_2 photocatalyst synthesised by CVD method. Langmuir. 2000;16:6216–6222. doi:10.1021/la000119l
38. Wang CC, Zhang Z, Ying JY. Photocatalytic decomposition of halogenated organics over nanocrystalline titania. Nanostruct Mater. 1997;9:583–586. doi:10.1016/S0965-9773(97)00130-X
39. Burns A, Li W, Baker C, Shah SI. Sol-gel synthesis and characterization of neodymium-ion doped nanostructured titania thin films. Mater Res Soc Sym. 2002;703:193–197.
40. Coville NJ, Tshavhungwe AM. Mesoporous ethanesilica materials with bimodal and trimodal pore-size distributions synthesised in the presence of cobalt ions. S Afr J Sci. 2010;106(7/8), Art. #213, 5 pages. doi: 10.4102/sajs.v106i7/8.213
41. Wang Y, Chen S-G, Tang XH, et al. Mesoporous titanium dioxide: Sonochemical synthesis and application in dye-sensitized solar cells. J Mater Chem. 2001;11:521–526. doi:10.1039/b006070o
42. Huang W, Tang X, Wang Y, Koltypin Y, Gedanken A. Selective synthesis of anatase and rutile via ultrasound irradiation. Chem Commun. 2000;15:1415–1416. doi:10.1039/b003349i
43. Yu JC, Zhang LZ, Yu JG. Direct sonochemical preparation and characterization of highly active mesoporous TiO_2 with a bicrystalline framework. Chem Mater. 2002;14:4647–4653. doi:10.1021/cm0203924
44. Oh CW, Lee GD, Park SS, Ju CS, Hong SS. Synthesis of nanosized TiO_2 particles via ultrasonic irradiation and their photocatalytic activity. React Kinet Catal Lett. 2005;85:261–268. doi:10.1007/s11144-005-0269-3
45. Tian B, Chen F, Zhang J, Anpo M. Influences of acids and salts on the crystalline phase and morphology of TiO_2 prepared under ultrasound irradiation. J Coll Interface Sci. 2006;303:142–148. doi:10.1016/j.jcis.2006.07.023, PMid:16890236
46. Liu Y, Li Y, Wang Y, Xie L, Zheng J, Li X. Sonochemical synthesis and photocatalytic activity of meso- and macro-porous $TiO_{(2)}$ for oxidation of toluene. J Hazard Mater. 2008;150:153–157. doi:10.1016/j.jhazmat.2007.04.088, PMid:17560714
47. Neppolian B, Wang Q, Jung H, Choi H. Ultrasonic-assisted sol-gel method of preparation of TiO_2 nanoparticles: Characterization, properties and 4-chlorophenol removal application. Ultrason Sonochem. 2008;15:649–658. PMid:18024153
48. Yang K, Zhu J, Huang S, Zhu X, Ma G. Sonochemical synthesis and microstructure investigation of rod-like nanocrystalline rutile titania. Mater Lett. 2003;57:4639–4642. doi:10.1016/S0167-577X(03)00376-8
49. Latt KK, Kobayashi T. TiO_2 nanosized powders controlling by ultrasound sol–gel reaction. Ultrason Sonochem. 2008;15:484–491. doi:10.1016/j.ultsonch.2007.08.001, PMid:17904404
50. Mahmoud MA, Poncheri A, Badr Y, Abd El Wahed MG. Photocatalytic degradation of methyl red dye. S Afr J Sci. 2009;105:299–303.